

SELF-EXCITED TORSIONAL OSCILLATIONS
OF AN AIRFOIL

Thesis by
Charles N. Levy

In Partial Fulfillment of the Requirements
for the Degree of Aeronautical Engineer

California Institute of Technology
Pasadena, California

June 1945

ACKNOWLEDGEMENT

The author would like to express his appreciation to Professor Louis G. Dunn under whose guidance this research was performed, to Mr. Morton Finston for his assistance, and to members of the Laboratory staff for their aid in manufacturing the suspension system and operation of the tunnel.

TABLE OF CONTENTS

| PART | | PAGE |
|-------|----------------------------------|------|
| I. | SUMMARY | 1 |
| II. | INTRODUCTION | 2 |
| III: | DESCRIPTION OF APPARATUS | 4 |
| | Test Procedure | 8 |
| | Accuracy | 10 |
| IV. | EXPERIMENTAL RESULTS | 11 |
| V. | DISCUSSION | 13 |
| | Existing Theory | 13 |
| | Conclusions | 15 |
| | Suggestions for Further Research | 17 |
| VI. | NOTATION | 18 |
| VII. | REFERENCES | 19 |
| VIII. | FIGURES AND GRAPHS | 21 |

I. SUMMARY

This thesis is a report on one phase of a program on the self-excited oscillations of an airfoil. This program was sponsored by the National Advisory Committee for Aeronautics at the California Institute of Technology. This thesis covers the torsional oscillations of an elastically suspended airfoil.

The experimental work consisted of measurements of the amplitude of torsional oscillations of a wing elastically suspended in the airstream of a wind tunnel so as to be capable of torsional oscillations only. The results show that torsional oscillations occur at all velocities above a critical velocity and increase in amplitude with velocity without reaching any apparent limit.

Glauert's theory of the forces on an oscillating airfoil do not agree with the experimental results obtained. This theory indicates that oscillations below the stall will not occur for the values of V/nb studied here, whereas the experiments indicate that oscillations do exist.

II. INTRODUCTION

Investigation of the failure of the Tacoma Narrows bridge indicated that a flat plate would exhibit self-excited torsional oscillations of rather large amplitude. A previous investigation¹ showed that self-excited bending oscillations of the NACA 0006 and 0012 airfoils do occur. This thesis is an extension of reference 1 to the case of torsional oscillations.

The oscillations reported here differ from normal types of flutter in that they are steady oscillations that do not involve coupling of several degrees of freedom. The experiments to be described are all one degree of freedom oscillations.

No experiments identical to the ones performed here have been noted in the literature. Bollyay and Brown² made experiments in which the airfoil was forced to oscillate by electro-mechanical means. However, in this case the airfoil motion was a combined oscillation and translation and the axis of oscillation was fixed by the suspension system. Reid and Vincenti³ made measurements of the lift ratio and the phase angle between the lift and the motion of an airfoil performing torsional oscillations. Silverstein and Joyner⁴ made measurements of the phase angles for low V/nb with existing theory was noted, but discrepancies were found for large values of V/nb . Reid and Vincenti found qualitative agreement with theory for the ratio of oscillating lift to steady state lift.

The airfoil theory for non-uniform motion has been worked out by several authors. Glauert⁵ has considered the case of pure torsional oscillations for infinite aspect ratio in detail and has paid special attention to the damping moment. Kármán and Sears⁶ have obtained similar results more simply and have considered translational oscillations and rotational oscillations about the midpoint of the airfoil. Their results could be extended to cover the cases investigated here and in reference 1. Sears⁷ has extended the theory to the case of finite span airfoils. Durand⁸ discusses Glauert's results rather thoroughly.

III. DESCRIPTION OF APPARATUS

The main items of apparatus used are the same as in reference 1; only the suspension system is different. However a short resume of all the apparatus will be given.

The wind tunnel used in this investigation is an open return type with a 36x42 inch semi-octagonal working section. Power is provided by an eight-cylinder gasoline motor of 125 horsepower. An eight-bladed, four foot fan designed to give a test section speed of 90 miles per hour is driven by the motor. A sketch of the tunnel is given in Fig. 1. The three screens in front of the contraction are used to attain smooth, uniform flow in the test section.

The OOL2 airfoil used in this investigation is of laminated wood construction with a 9 inch chord and 41 inch span. The ends of the airfoil are fitted with dural blocks that receive the pins connecting the airfoil to the suspension system.

Two suspension systems were used for the torsion tests. The first system, simple in construction, was intended to be used to study the general nature of the oscillations rather than to obtain accurate measurements. This system consisted of mounting the airfoil on helical tension springs, four to a side, as shown in Figure 3 of reference 1. The spacing and stiffness of the springs were such that the torsional and vertical frequencies were quite different so that the airfoil could oscillate in pure torsion. The airfoil

was theoretically capable of choosing its own axis of oscillation. However, since the aerodynamic forces were small compared to the spring forces, the actual axis of oscillation was almost midway between the springs at 37% of the airfoil chord. Measurements of the oscillations were made by attaching pointers to the airfoil and measuring the amplitude of the pointer ends. The measurements are not very accurate since considerable parallax results from a necessary horizontal displacement of almost 1/2 inch between pointer and scale and the difficulty of visual observation of the oscillation limits.

The second suspension system was designed to enable greater precision of measurement and accuracy of results. In order to eliminate mechanical friction and damping as well as to attain a linear spring force it was decided to use an aluminum rod as the torsion spring. The use of this type of torsion spring eliminates friction entirely and introduces only the internal damping of the material. In order to attain the largest element possible consistent with the required strength, 24ST was selected as the alloy. This alloy has a proportional limit in torsion somewhat greater than the linear range of the strain gauge used and has a low modulus of rigidity. The torsion rod is fitted with two integral flanges. The outer flange of the rod is fastened by screws to a heavy steel tube. The inner end of this tube is silver soldered to a steel plate that is drilled so as to operate as a protractor. The lower end of the

protractor is pivoted on a screw that fastens the lower end to the lower support beam. The upper end of the protractor is drilled with a series of holes so that the airfoil can be adjusted to any angle of attack from 0° to 30° by 1° increments. The inner flange of the torsion rod is fastened by screws to a steel beam. This beam is provided with several sets of holes in order to allow the airfoil to be shifted relative to the axis of oscillation. That a very low mechanical damping is introduced by this system of suspension is evidenced by the fact that it takes over four minutes for a disturbance to damp out when no airfoil is in place and about two minutes with the airfoil in place and the air speed at zero velocity.

Since there did not seem to be any advantage to be gained from the use of multiple strain gauges in this case, only one strain gauge was used. This gauge was wrapped around one of the torsion rods at a 45° angle to the rod axis. Thus the gauge responds to the normal stresses induced by the twisting of the rod. The output from the strain gauge is amplified and then recorded on an oscillograph (Heiland Type A-400R6). The oscillograph has a timer that marks $1/100$ second intervals so that frequency measurements can be made. The gain of the amplifier-oscillograph combination is flat within 1% for frequencies from 5-40 cycles per second.

In order to obtain the absolute amplitude of the

oscillations, a scratch was made on the attaching beam and the vertical amplitudes measured with the telescopic device of reference 1 (figure 7) for low amplitudes (up to 2°) and an ordinary scale for large amplitudes (2° to 9°).

Test Procedure

Since the gain of the amplifier-oscillograph combination may change with time, calibration is necessary before and after each set of runs. This is done by shunting a fixed resistor across the strain gauge and making a record of the transient response. Comparison of the maximum amplitude of the recorded response gives a relative calibration that can be used to compare the various records.

With the angle of attack set to the desired value, the velocity was increased from a low value by moderate increments until oscillations were obtained. A record of the oscillations was made and then the velocity changed slightly. Another recording was then made. This process was repeated until sufficient points to define a **amplitude-velocity** curve was obtained. It was necessary to be careful in taking the records to make sure that the oscillation was as large as could be obtained since preliminary tests showed that two modes of motion were possible at some angles of attack. At any airspeed at which oscillation occurs, it is possible to find a large and a small amplitude. The small amplitude oscillation can be obtained by stopping the airfoil and then allowing it to oscillate again. The large oscillation can be obtained by giving the airfoil an initial torsional oscillation of sufficient magnitude. If the initial amplitude is not large enough, the motion quickly damps to the small oscillation. Normal operating procedure was to increase the velocity slowly until the maximum velocity was attained and

then decrease the velocity taking several check points on the way down. For most angles of attack, no difference was noted between those points made with increasing velocity and those made with decreasing velocity. The main difference noted was that oscillations could be obtained at lower velocities as the velocity was decreased than could be obtained with increasing velocity.

Accuracy

The amplifier-oscillograph combination will give an accuracy of 2% from 5-40 cycles per second. The error in reading the records is approximately 2% for normal amplitudes. Therefore the mechanical error is about 4% total.

The calibration of the record with the absolute amplitude shows an accuracy of 5%.

There is one other difficulty of measurement that should be mentioned. The average time allowed between points was one minute for the 2.6 cycle oscillation and two minutes for the 4.3 cycle oscillation. Visual observation and some check records indicated that this time was adequate. However, it may be that in some cases a longer period should have been allowed for the oscillation to become steady.

It should be noted that for 86% axis position at angles of attack of 8° and 9°, the frequencies noted are considerably below the 5 cycle limit for uniform response of the amplifier.

IV. EXPERIMENTAL RESULTS

Preliminary tests were made with the helical spring suspension with the axis of oscillation at approximately 37%. With this suspension, the axis of oscillation was not fixed and some small variations may have occurred. However, no change of axis was noted visually. Curves of amplitude vs V/nb are not given here since sufficient data to establish the zero point of the oscillation only were obtained. A plot of α_g vs $(V/nb)_c$ is given for this data in fig. 15. The frequency as determined by a strobotac was 13.8 cycles/sec.

With the final suspension system, three different axes of oscillation were investigated. Most of the data was taken with the axis of oscillation located at 38% of the chord. Additional data was taken with the axis of oscillation at 36% of the chord. A forward axis location of 11% chord ahead of the leading edge was investigated at angles of attack of 16° and 20° . There was some spasmodic motion of the airfoil of small amplitude, but no regular oscillations as observed at the other two axes of oscillation.

The 38% axis position showed oscillations as low as $\alpha_g = 10^\circ$. Tests at $\alpha_g = 9^\circ$ showed no steady oscillations. At $\alpha_g = 10^\circ$ (fig. 5), the curves of angular amplitude vs V/nb are characterized by starting initially as a linear variation followed by a region of approximately constant amplitude and then having a second region of linear response.

The 86° axis position showed oscillations as low as $\alpha_g = 8^\circ$. At $\alpha_g = 7^\circ$ spasmodic motions of almost 1° amplitude were obtained. The results were similar to that observed at $\alpha_g = 3^\circ$ before the larger steady oscillations were obtained. The amplitude vs V/nb graphs show a linear variation with V/nb for angles of attack above 12° (fig. 7-13). The amplitude curves for 3° and 9° are shown in fig. 3 and 4. Enough points to establish the variation of amplitude with V/nb have not been obtained. Also, the frequency at some points was so low that the error caused by the decrease in amplifier response may be rather large. Therefore, the curves drawn for these angles should be taken as approximate only. For these angles it seems that small oscillations in the range of 0.4° to about 3° for $\alpha_g = 8^\circ$ (fig. 3) cannot be obtained. Attempts to do so resulted in irregular oscillations. The same thing occurs for 0.6° to 2.6° for $\alpha_g = 9^\circ$ (fig. 4). Also for these angles there is a considerable frequency variation with V/nb . The results are shown in fig. 14. No such variation was noted at any other combination of axis position and angle of attack.

It should be pointed out that, at both axis positions investigated, the amplitude increases continuously with increasing wind velocity differing from the case of the bending oscillations observed in reference 1.

V. DISCUSSION

Existing Theory

The airfoil theory for non-uniform motion has been developed by a number of authors. Glauert⁵ has investigated the particular case of an airfoil of infinite aspect ratio oscillating about an arbitrary point of the chord. The conclusions are that the damping moment is positive except for hinge positions further forward than 25% of the chord where the damping moment is negative for low frequencies.

Glauert's results are

$$C_{m_H} = -2\pi(1/4 - x/b)\alpha_0 - 2\pi f d_1 \sin nt - \frac{4\mu}{V/b} \cos nt$$

where

$$f = f(V/b)$$

$$\mu = \mu(V/b)$$

and where the oscillation has been assumed to be

$$d = d_0 + d_1 \sin nt$$

then

$$\frac{dd}{dt} = n d_1 \cos nt$$

$$\frac{d^2d}{dt^2} = -n^2 d_1 \sin nt$$

Making this substitution we get

$$C_{m_H} = -2\pi(1/4 - x/b)\alpha_0 + \frac{2\pi f}{n^2} \frac{d^2d}{dt^2} - \frac{4\mu b}{V} \frac{dd}{dt}$$

The suspension system used is a one degree of freedom system and the equation of motion under a forced oscillation (neglecting the damping of the suspension) is

$$I \frac{d^2\alpha}{dt^2} + k\alpha = C_{m_H} \frac{\rho}{2} b^2 V^2$$

or

$$\left[I - \frac{2\pi f}{n^2} \frac{\rho}{2} b^2 V^2 \right] \frac{d^2\alpha}{dt^2} + \frac{4\mu b}{V} \frac{\rho}{2} b^2 V^2 \frac{d\alpha}{dt} + k\alpha = -2\pi \frac{\rho}{2} b^2 V^2 (1/4 - x/b) \alpha_0$$

Thus we see that the aerodynamic forces on the airfoil due to oscillation cause an additional apparent moment of inertia and a damping moment. The right hand side of the equation is the steady moment that would occur if the airfoil were not oscillating. It is seen that the damping moment is positive if μ is positive. From Glauert's paper the smallest value of V/nb for which μ becomes negative is estimated to be approximately 40 and then μ becomes negative only for hinge points less than $x/b = 25\%$. For the 38% and 86% axes of oscillation investigated, μ would always be positive. The additional apparent moment of inertia would cause a change of frequency of oscillation. Experimentally, variation of frequency of oscillation was noted only for the case of the axis of oscillation at 86% and at 8° and 9° angle of attack. This frequency variation is plotted in fig. 14 against V/nb .

Conclusions

The first thing to be noticed about these tests is that the Reynolds number is $59,000 < R < 200,000$. Under static conditions, this low Reynolds number causes the airfoil to stall much earlier than normal. It is estimated that the 0012 airfoil will have a $C_{l_{max}} = 0.80$ and a stalling angle of attack of 11° for a Reynolds number of $100,000^9$: However this is not the whole story of the airfoil stall Farren¹⁰ has shown that for an airfoil whose angle of attack is varying with time an "overlift" of as much as 50% can occur if the angle of attack is varying rapidly enough. Thus for the 0012 at $R=100,000$, $C_{l_{max}} = 1.20$ and the stalling angle of attack = 13° for very rapid changes of angle of attack. In the case of an airfoil performing torsional oscillations slightly above the static stall, it is possible that the airfoil, although originally stalled before oscillations start, may not be stalled during oscillation. Above 13° it would seem that the airfoil would always be in the stalled state, although it would take wake surveys to prove the stalling angle and the character of the wake.

It should be noted that for oscillations above the stall, an airfoil has static instability¹². This static instability is caused by the negative slope of the lift curve. Thus self-excited oscillations would be expected to occur above the airfoil stall.

For the Reynolds numbers at which these tests are made, it is expected that in the wake near the trailing edge of the airfoil a Karman vortex street¹¹ would be formed although the street should rapidly become turbulent at large distances from the trailing edge. The frequencies with which the vortices are shed from a body can be computed from

$$\frac{n b \sin \alpha_g}{V} = K$$

where K is the Karman number. The experimental values of K vary from 0.15 to 0.21 for airfoils and 0.148 to 0.18 for flat plates for angles of attack greater than 30°. ¹¹

The results of reference 2 indicate that oscillations start when the vortex frequency coincides with the natural frequency of the wing. If this is assumed then K can be calculated from the above equation. The results of this calculation are shown in fig. 17 as a function of α_g . It appears that for the axes positions and frequencies of $x/b = 38\%$, $n=8.6$ and $x/b = 37\%$, $n=13.8$, the variation of K with α_g is linear and then reaches a maximum value. For the 86%, $n=4.3$ axis position and frequency the lowest angles of attack of 8° and 9° are not plotted since the curves are not accurate enough to define the starting velocity. The maximum value of K is 0.180 and occurs at the $x/b = 37\%$, $n=13.8$ configuration for an angle of attack of 23°. For $x/b=38\%$, $n=8.6$ the maximum value of K is 0.168 and occurs at 20°. For the 86% axis position the maximum value of K had not yet been attained when the angle of attack was 24°. These maximum values are within the limits given by reference 11 for airfoils.

Suggestions for Further Research

The present experimental results are concerned with the amplitude of the oscillations and their variation with wind velocity. The next stage appear to be the determination of the damping. After this is completed, wake surveys and boundary layer measurements should be made in order to determine the mechanism causing these oscillations.

Notation

- α_g = angle of attack with reference to the centerline of the tunnel.
- x/b = hinge position aft of the leading edge, percent chord.
- C_{mH} = pitching moment coefficient about axis of oscillation.
- f, μ = parameters used in the Glauert analysis.
- I = moment of inertia about axis of oscillation.
- k = torsional spring constant.
- K = dimensionless Karman number.
- $(V/nb)_c$ = value of V/nb at which oscillations begin
- V/nb = inverse of reduced frequency.
- V = wind velocity.
- n = frequency of oscillations.
- b = airfoil chord.

References

1. Dunn and Finston, "Self-Excited Oscillations of Airfoils", Report in Final Fulfillment of Contract NAW2329 April, 1945. California Institute of Technology. Confidential
2. Bolloy and Brown, "Some Experimental Results on Wing Flutter," Journal of the Aeronautical Sciences, Vol. 8 No. 8, June 1941 pg. 312
3. Reid and Vincenti, "An Experimental Determination of the Lift of an Oscillating Airfoil", Journal of the Aeronautical Sciences; Vol 8, No 1, November 1940 Pg. 1
4. Silverstein and Joyner, "Experimental Verification of the Theory of Oscillating Airfoils", N.A.C.A Technical Report No. 673, 1939
5. Glauert, "The Force and Moment on an Oscillating Airfoil", Aeronautical Research Committee, Reports and Memoranda No. 1242, 1930
6. Karmann and Sears, "Airfoil Theory for Non-Uniform Motion", Journal of the Aeronautical Sciences, Vol. 5, No. 10, August 1938 Pg. 379
7. Sears, "A Contribution to the Airfoil Theory for Non-Uniform Motion", Proceedings of the Fifth International Congress of Applied Mechanics 1938. Pg. 483
8. Durand, "Aerodynamic Theory" Julius Springer, Berlin 1934 Vol.II Chap.V. Contains Bibliography and Glauert's results.
9. Jacobs and Sherman, "Airfoil Section Characteristics as affected by Variations of the Reynolds Number", N.A.C.A Technical Report No. 586, 1937

10. Farren, "Reaction on a Wing whose Angle of Incidence is Changing Rapidly", A.R.C. Reports and Memoranda No. 1648, Jan. 1935
11. Goldstein, "Modern Developments in Fluid Dynamics", Oxford, 1938 Vol. II Chaps. XIII
12. Den Hartog, "Mechanical Vibrations", Mc Graw-Hill, First Edition 1934 Pg. 301.

CONFIDENTIAL

ATTACHMENT PLUG

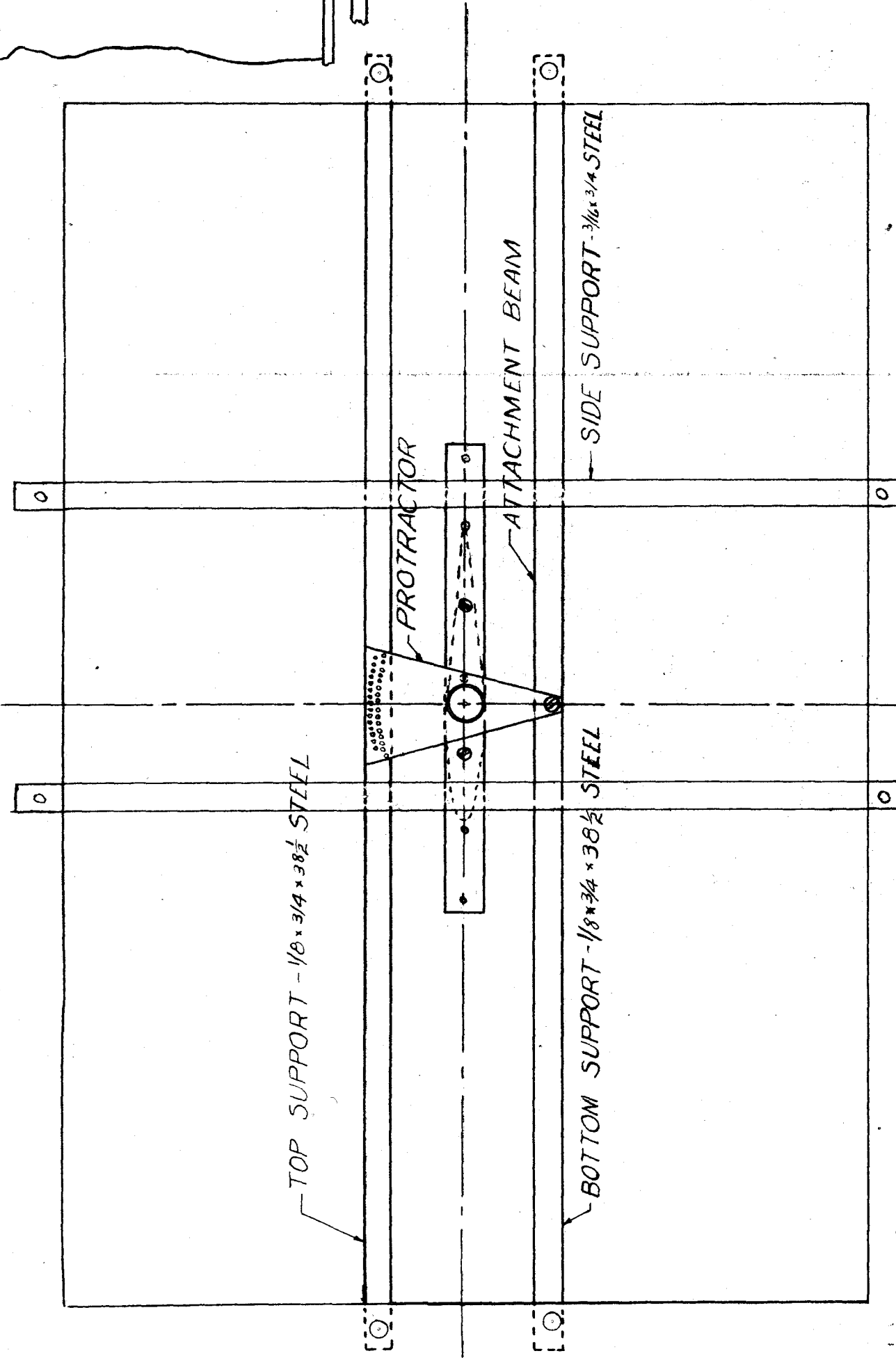
ATTACHMENT PIN

1/16 x 1/4 STEEL

SILVER
SOLDERED

TORSION SPRING
0.190 DIA 245T

SUPPORT TUBE
1 x .065 x 3 STEEL



SIDE VIEW OF INSTALLATION
SCALE: 1/4 SIZE

TOP VIEW OF TORSION SPRING
SCALE: FULL SIZE

CONFIDENTIAL

| | | | | | |
|--------------------------------------------------------------------------|-----------|--------------------------------|---------|----------|----------|
| TOLERANCES ±.010 OR 1/32 UNLESS OTHERWISE NOTED | | SCALE NOTED | | REF. | |
| 5-15-45 | C.N. LEVY | DRAFTSMAN | CHECKED | APPROVED | ENGINEER |
| GUGGENHEIM AERONAUTICAL LABORATORY CALIFORNIA INSTITUTE OF TECHNOLOGY | | TORSIONAL OSCIL. SUSPENSION | | | |
| NAME | | DRAWING NO. | | | |
| | | FIG. 2 | | | |

NACA 0012 AIRFOIL
AMPLITUDE RESPONSE AS A FUNCTION OF V/hb
TORSIONAL OSCILLATIONS

$\alpha_0 = 5^\circ; X/b = 0.6 \%$

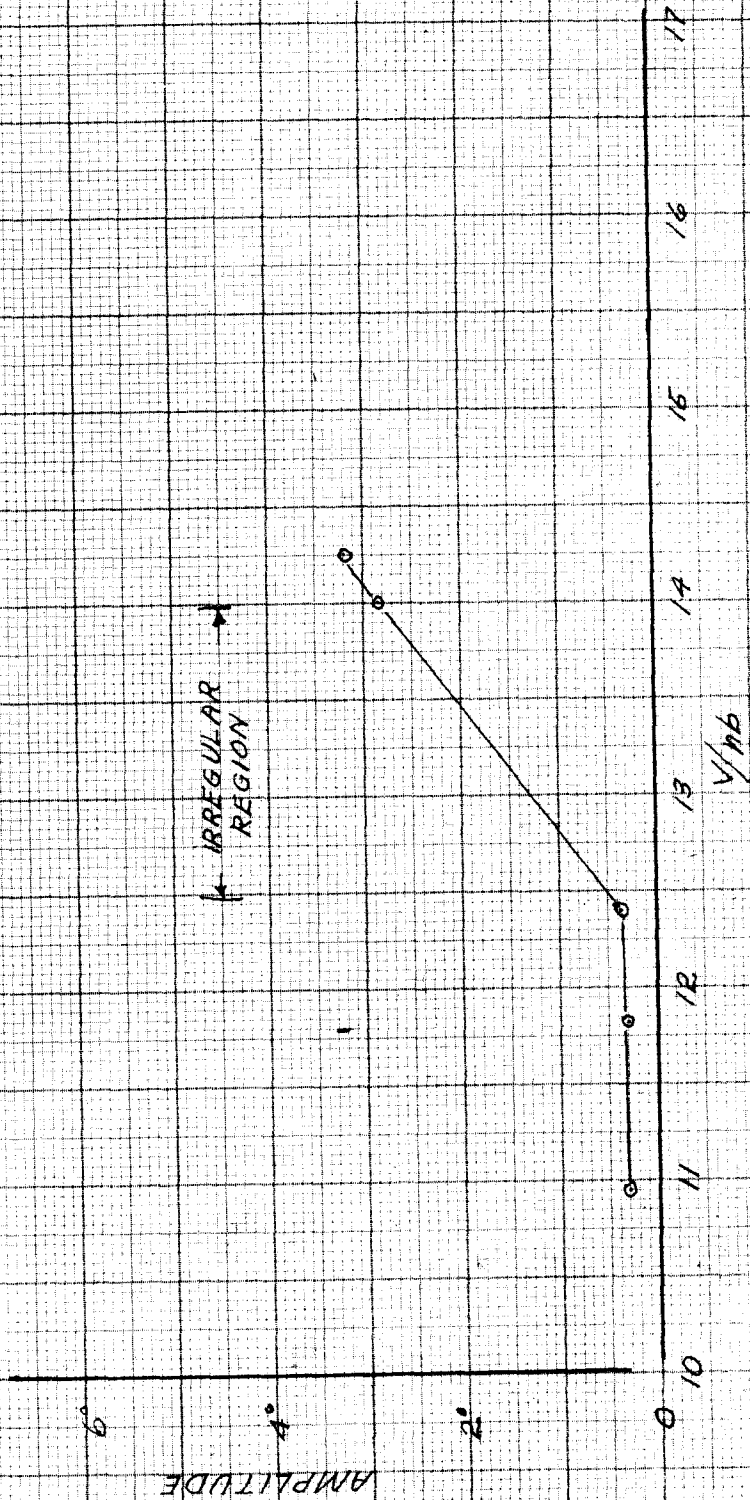


FIG. 3

NACA 0012 AIRFOIL
AMPLITUDE RESPONSE AS A FUNCTION OF V/m_b
TORSIONAL OSCILLATIONS

$\alpha_0 = 0^\circ$; $x/b = 0.67$

AMPLITUDE

AMPLITUDE

IRREGULAR
REGION

V/m_b

FIG. 4



0
2
4
6

10
11
12
13
14
15
16

NACA 0012 AIRFOIL
AMPLITUDE RESPONSE AS A FUNCTION OF V/nb
TORSIONAL OSCILLATIONS

$\alpha_g = 10^\circ$; $k/b = 38\%$

CONFIDENTIAL

○ VELOCITY INCREASING
○ " " DECREASING

AMPLITUDE

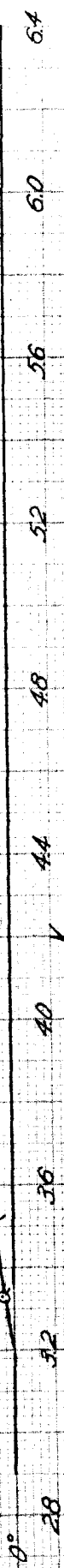


FIG. 5

NACA 0012 AIRFOIL
AMPLITUDE RESPONSE AS A FUNCTION OF $V/\omega b$
TORSIONAL OSCILLATIONS

$\alpha_0 = 11^\circ$; $X/b = 38\%$

○ VELOCITY INCREASING
○ " " DECREASING

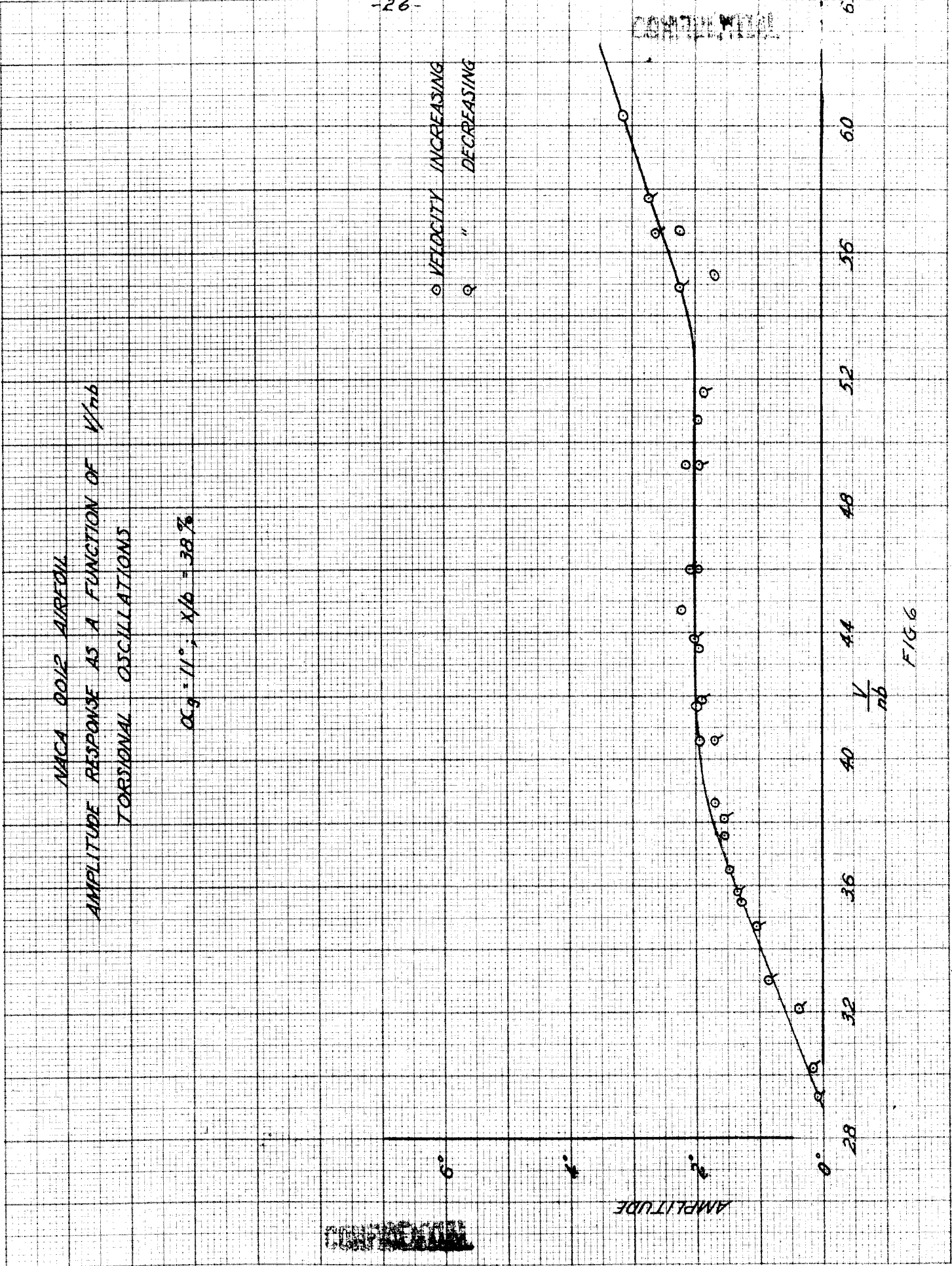
AMPLITUDE

0°
5°
10°

28 32 36 40 44 48 52 56 60 64

$V/\omega b$

FIG. 6



NACA 0012 AIRFOIL
AMPLITUDE RESPONSE AS A FUNCTION OF V/nb
TORSIONAL OSCILLATIONS

$\alpha_3 = 12^\circ; \chi/b = 38.7\%$

○ VELOCITY INCREASING
◐ VELOCITY DECREASING

AMPLITUDE

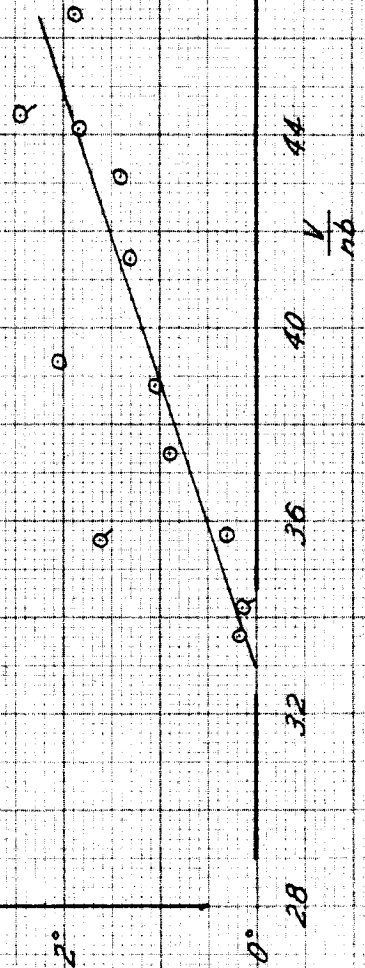


FIG. 7

NACA 0012 AIRFOIL
AMPLITUDE RESPONSE AS A FUNCTION OF V/nb
TORSIONAL OSCILLATIONS

$\alpha_g = 12^\circ$; $X/b = 66.7\%$

AMPLITUDE

0.6

0.5

0.4

0.3

VELOCITY INCREASING
↓
↑
VELOCITY DECREASING

58

62

66

70

74

78

82

86

90

94

V/nb

FIG. 8



NACA 0012 AIRFOIL
 AMPLITUDE RESPONSE AS A FUNCTION OF $V/\omega b$
 TORSIONAL OSCILLATIONS

$\alpha_g = 14^\circ$; $X/b = 38.7\%$

○ VELOCITY INCREASING
 ○ VELOCITY DECREASING

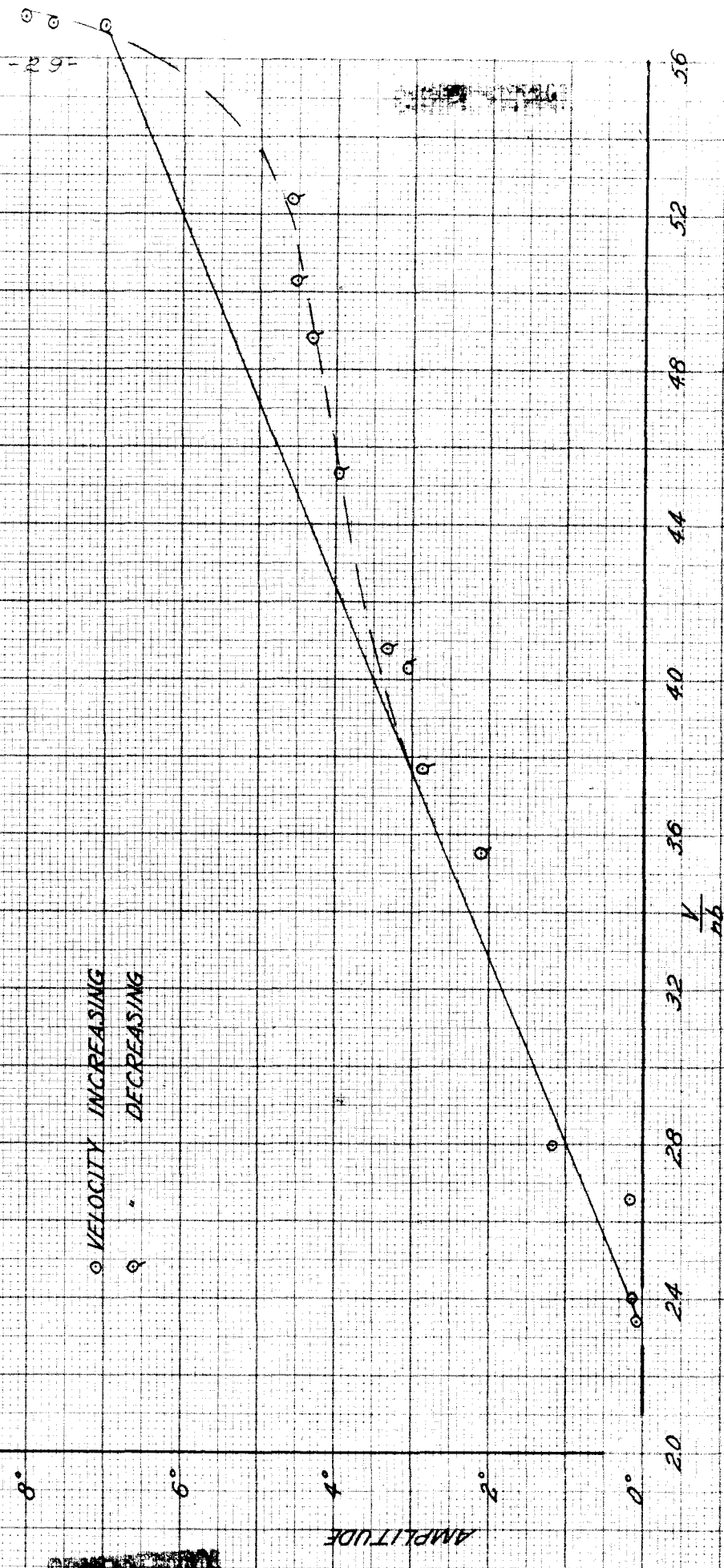


FIG. 9

NACA 0012 AIRFOIL
AMPLITUDE RESPONSE AS A FUNCTION OF V/b
TORSIONAL OSCILLATIONS

$\alpha_0 = 16^\circ$; X/b - NOTED

VELOCITY INCREASING
VELOCITY DECREASING

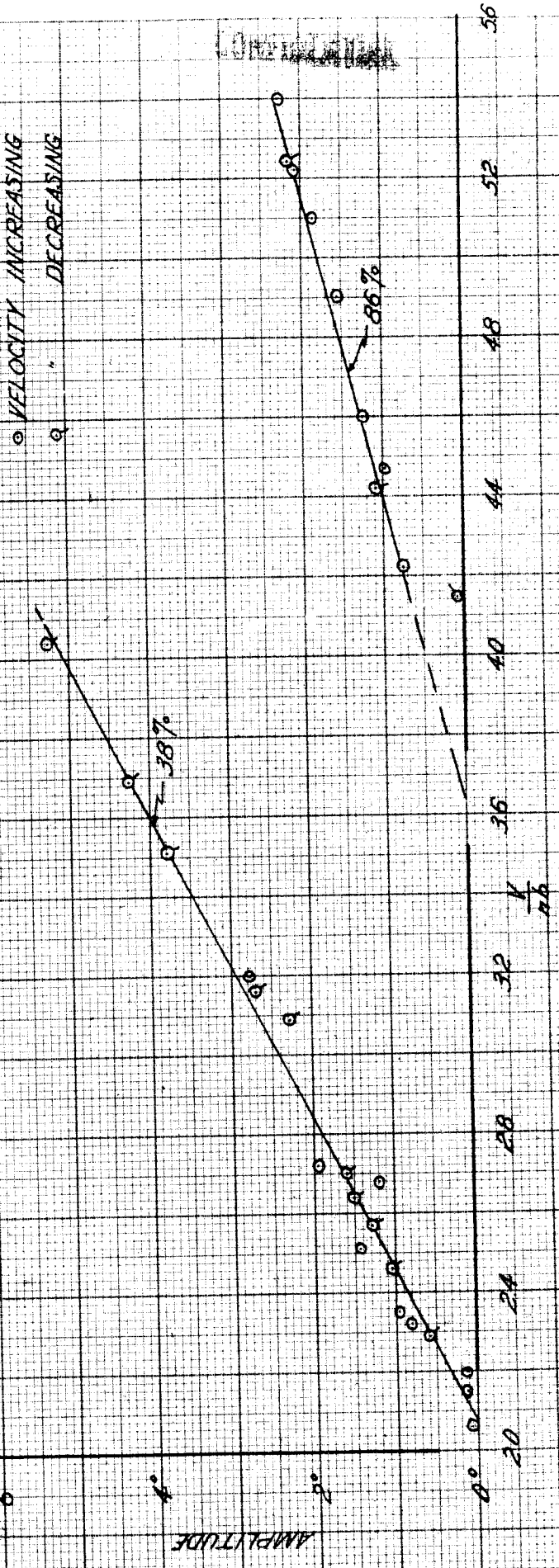


FIG. 10

NACA 0012 AIRFOIL
AMPLITUDE RESPONSE AS A FUNCTION OF $V/\alpha b$
TORSIONAL OSCILLATIONS

$\alpha_0 = 20^\circ$; X/b - NOTED

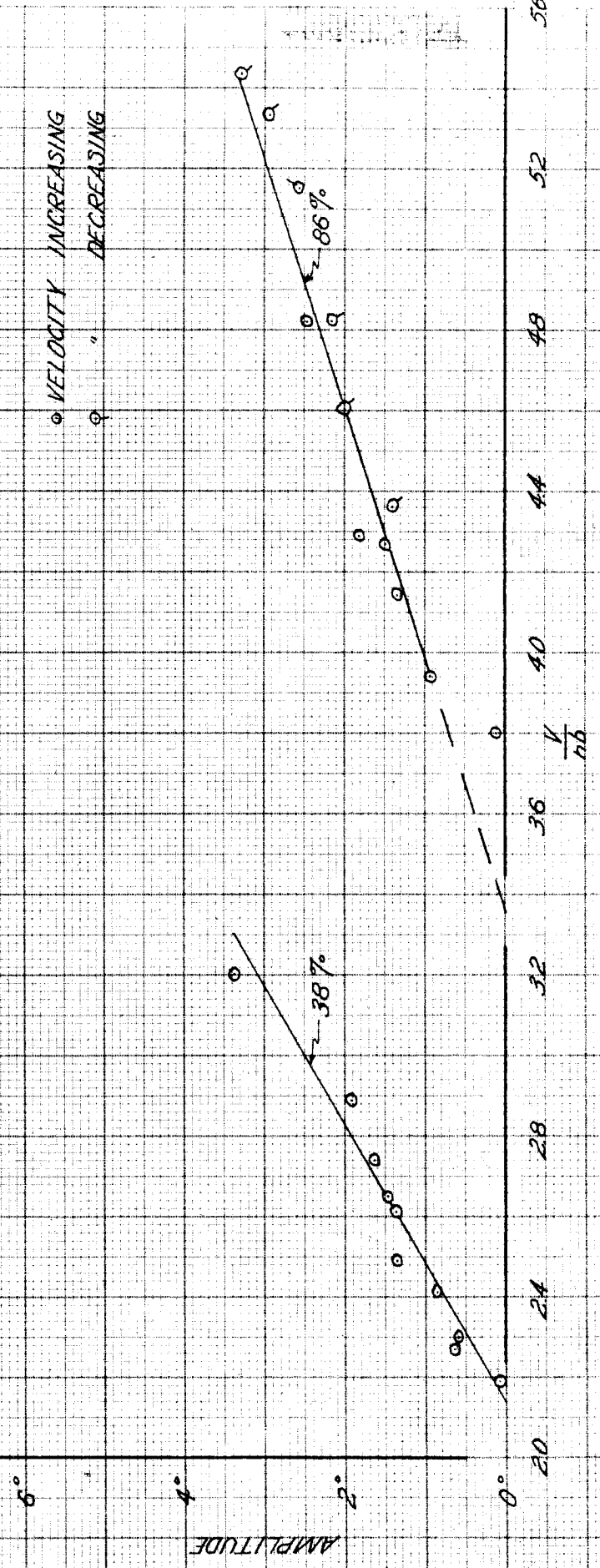


FIG. 11

NACA 0012 AIRFOIL
AMPLITUDE RESPONSE AS A FUNCTION OF $V/\omega b$
TORSIONAL OSCILLATIONS

$\alpha_g = 2.4^\circ$; X/b - NOTED

AMPLITUDE

6°
4°
2°
0°

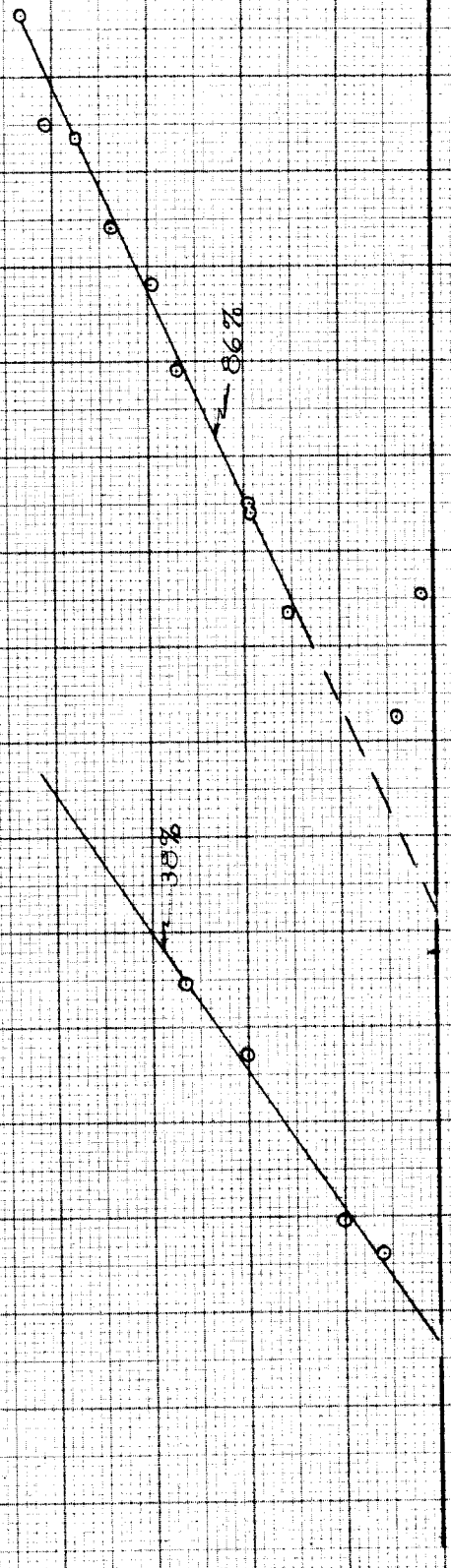


FIG. 12

NACA 0012 AIRFOIL
AMPLITUDE RESPONSE AS A FUNCTION OF V/nb
TORSIONAL OSCILLATIONS

$\alpha_0 = 28^\circ$; $X/b = 38\%$

CONFIDENTIAL

VELOCITY INCREASING

6°

AMPLITUDE

4°

2°

0°

20

24

28

32

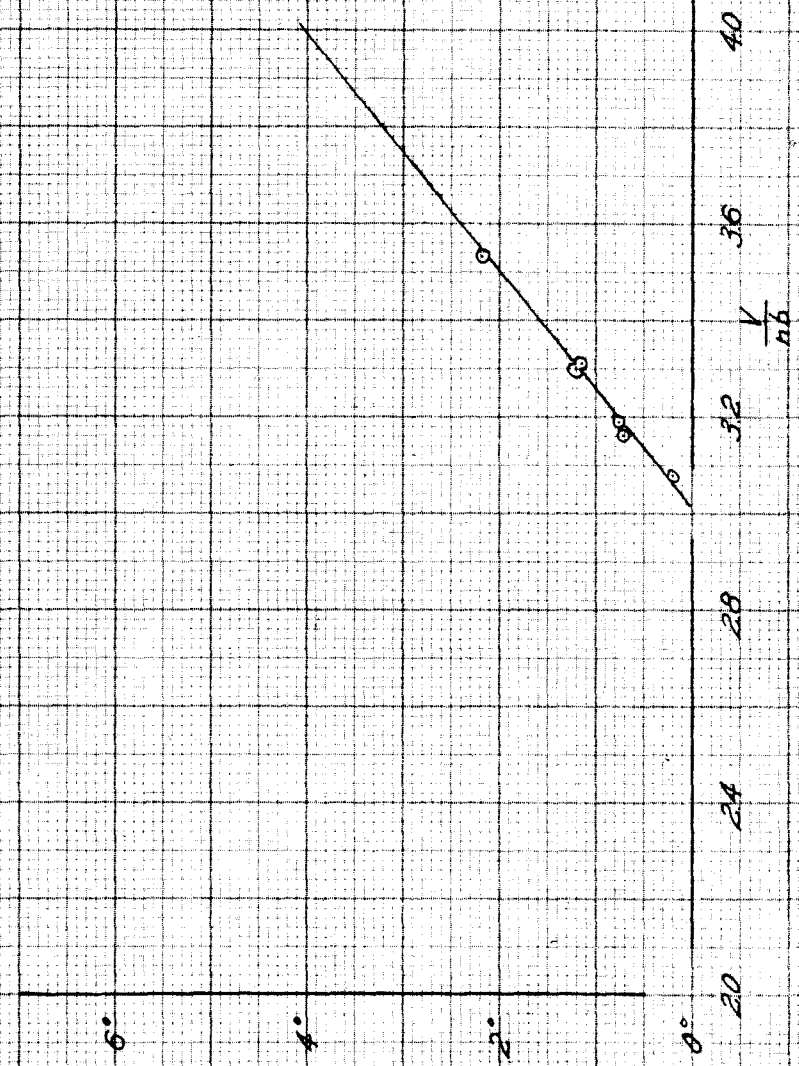
36

40

44

V/nb

FIG. 13



NACA FOUR AIRFOIL
FREQUENCY VARIATION WITH V/nb
TORSIONAL OSCILLATIONS

$\chi/b = 8.6\%$

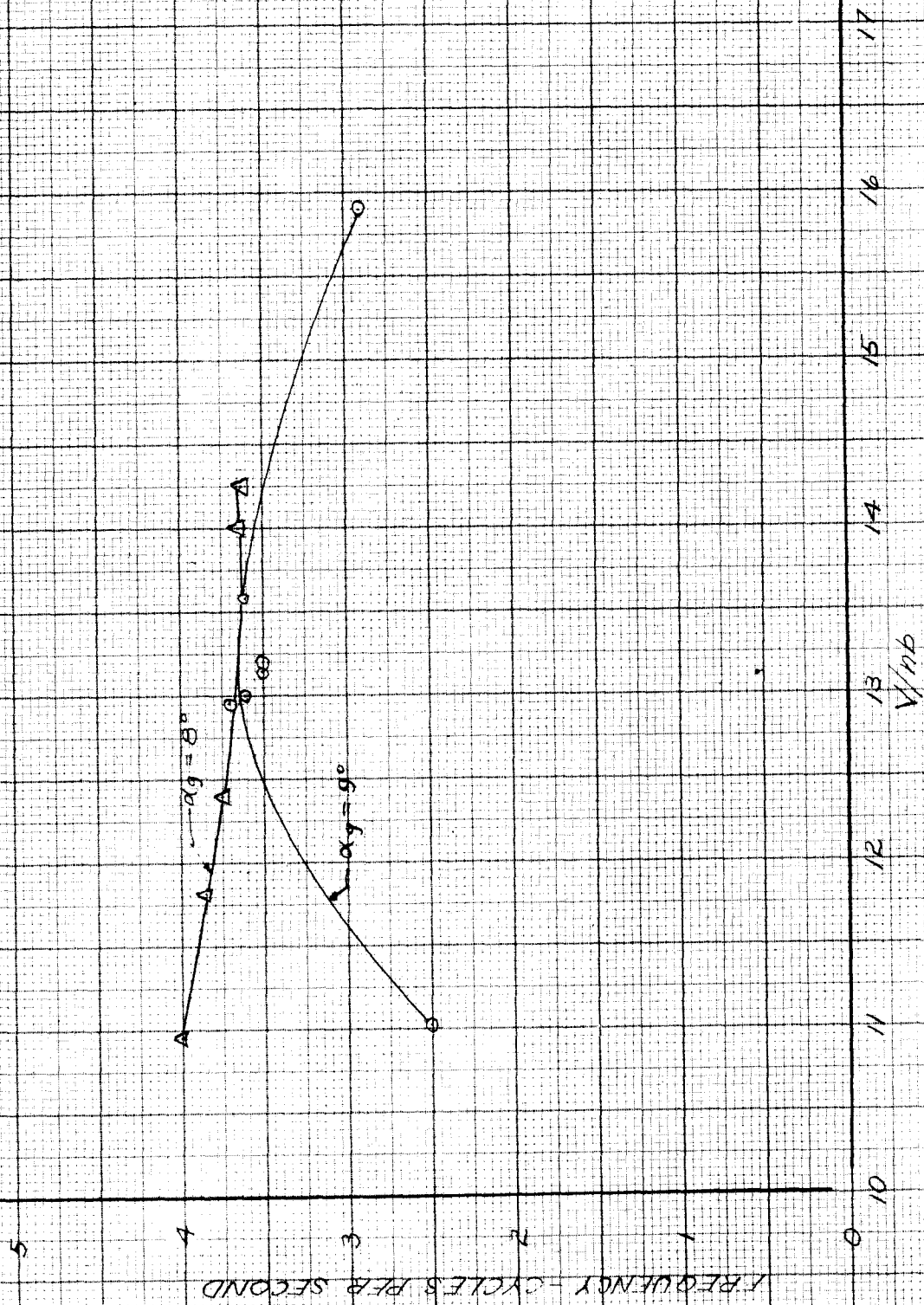


FIG. 14

NACA 0012 AIRFOIL
ANGLE OF ATTACK VS (V/V₀)_c
TORSIONAL OSCILLATIONS

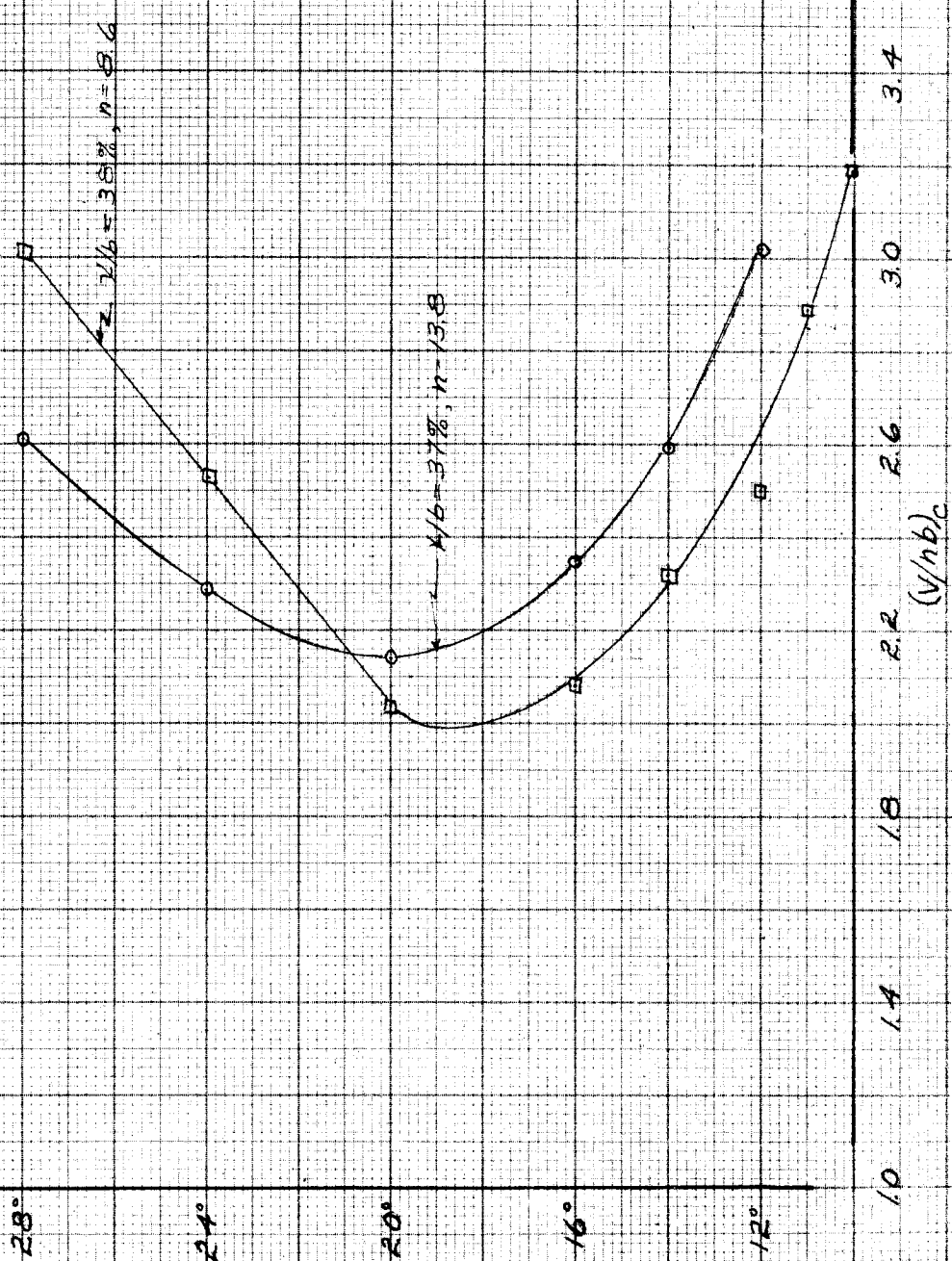
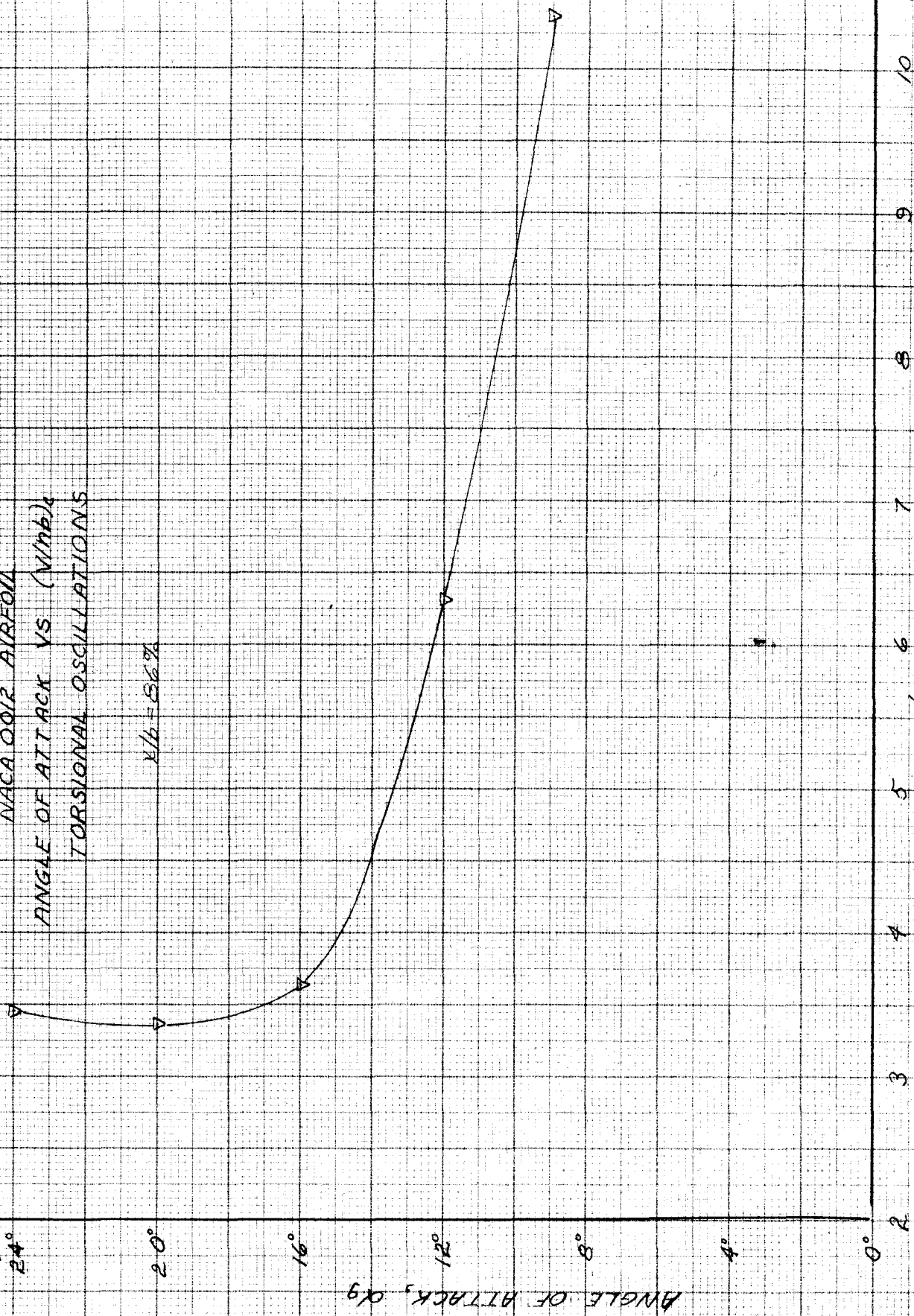


FIG. 15

NACA 0012 AIRFOIL
ANGLE OF ATTACK VS (V/nb)_c
TORSIONAL OSCILLATIONS

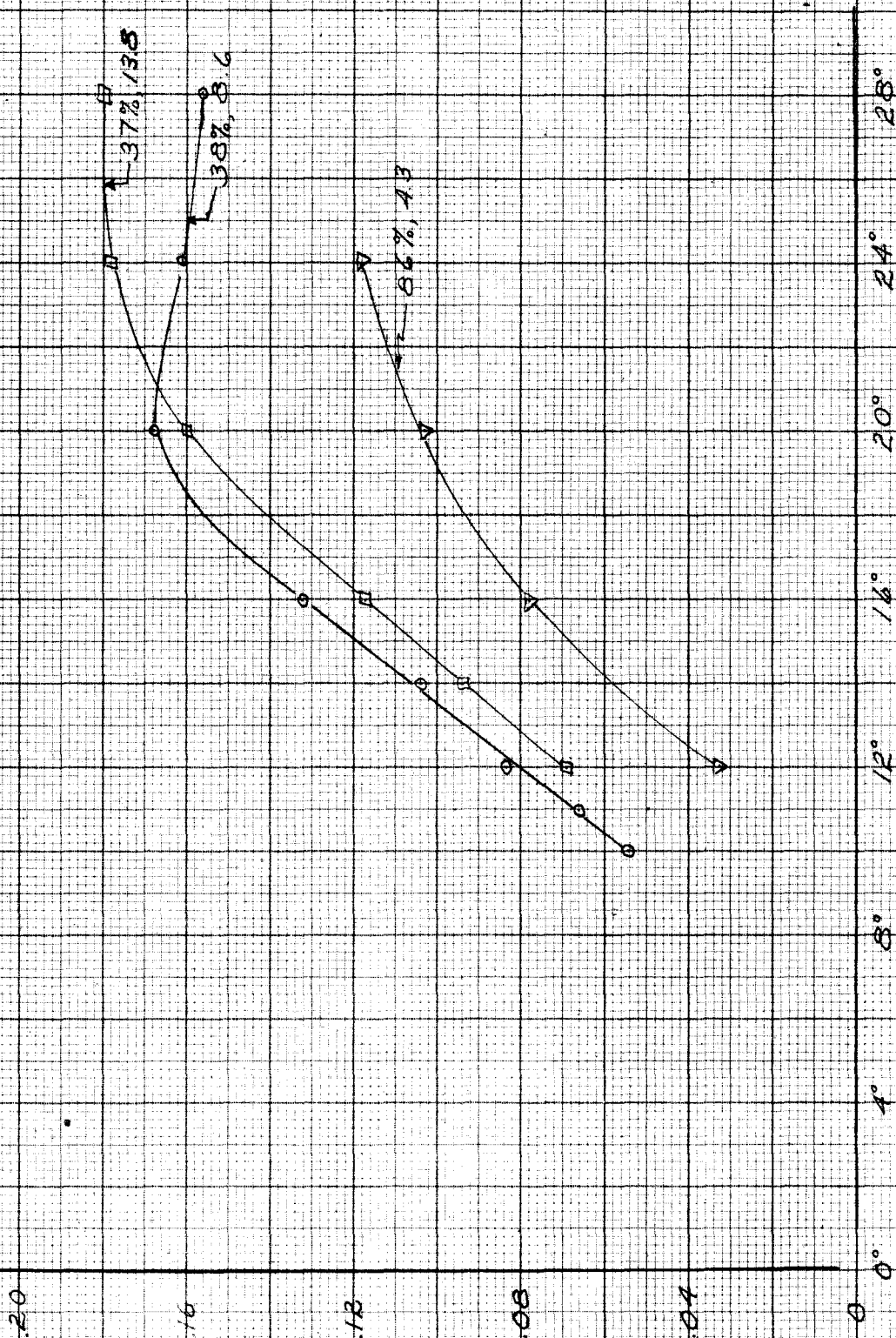
$\chi/b = 8.6\%$



(V/nb)_c
FIG. 16

CONFIDENTIAL

NACA 0012 AIRFOIL
KÁRMÁN CONSTANT VS α
TORSIONAL OSCILLATIONS



09 FIG. 17

K

CONFIDENTIAL